Justin M. Garwood[1], California Department of Fish and Wildlife, 5341 Ericson Way, Arcata, California 95521

Andrew G. Fountain, Department of Geology, Portland State University, P.O. Box 751, Portland, Oregon 92707

Kenneth T. Lindke, California Department of Fish and Wildlife, 5341 Ericson Way, Arcata, California 95521

Michael G. van Hattem, California Department of Fish and Wildlife, 619 2nd Street, Eureka, California 95501

and

Hassan J. Basagic, Department of Geology, Portland State University, P.O. Box 751, Portland, Oregon 92707

20th Century Retreat and Recent Drought Accelerated Extinction of Mountain Glaciers and Perennial Snowfields in the Trinity Alps, California

Abstract

The Trinity Alps is a compact glaciated subrange of the Klamath Mountains in northwest California with elevations < 2,750 m making it a unique location in the western US to study glacier change. We examined glacier change since the last Little Ice Age advance in the late 19th century by mapping historic glacier areas using clearly defined moraines. At least six glaciers existed in the Trinity Alps around the 1880s and estimated glacier cover was at least 55.4 ha (0.554 km^2). We tracked changes in two glaciers and two perennial snowfields since that time. Total glacier area decreased by 79% (43.8 ha to 9.1 ha) from the 1880s to 1994. By 2013, glacier area decreased another 7% of the 1880s area to 6.0 ha. Overall, retreat was similar for Salmon Glacier (–89%) and Grizzly Glacier (–84%), but since 1994 Salmon retreat has been much faster, 53% versus 16% for Grizzly. The extended 2012 to 2016 drought resulted in catastrophic retreat of both glaciers such that by 2015 Salmon Glacier disappeared and Grizzly Glacier retreated to 1.67 ha and partially stagnated, a –97% loss of total glacier area since the 1880s. Two snowfields (3.02 ha total area in 1955) were tracked since 1955, the Mirror Lake snowfield disappeared by the summer of 2013 and the Canyon Creek snowfield disappeared by October 2014. The unusually warm summer temperatures since 2005 combined with extremely low winter precipitation from 2013 to 2015 caused rapid retreat and near elimination of the Trinity Alps perennial snow and ice threatening local biodiversity that depends on these features.

Keywords: Klamath Mountains, glacier change, Little Ice Age, drought, California

Introduction

Glaciers and perennial snowfields (G&PS) respond to changes in snow accumulation and air temperature and are among the best indicators of regional climate change (Matthes 1935, Ahlmann 1953, Zemp et al. 2019). As global climate warms most G&PS shrink worldwide in response (Meier 1984, IPCC 2013, Radić et al. 2013, Zemp et al. 2015). One of the hydrological characteristics of glaciers and to a lesser extent, perennial snow, is that they act as frozen reservoirs of water within a watershed that release water during the warm summer months (Fountain and Tangborn 1985, Shook and Gray 1997, Frans et al. 2018). A hotter and drier summer causes G&PS to melt more, increasing downstream runoff. For this reason, G&PS are natural regulators of streamflow, buffering alpine watersheds against drought by maintaining aquatic and riparian dependent ecosystems during the summer and early autumn (Brown et al. 2007, Milner et al. 2017, McKernan et al. 2018).

Inventories of G&PS help to define how alpine hydrology and ecosystem response will change in the face of climate change (Robinson et al. 2001, Hall and Fagre 2003, O'Neel et al. 2015). For western North America, glaciers in Alaska and northwestern Canada have been losing mass at an

[1]Author to whom correspondence should be addressed.
Email: Justin.Garwood@wildlife.ca.gov

TABLE 1. The topographic characteristics of glaciers described in Oregon and California. Trinity Alps data are from inventory and measurements recorded during this study. Data for other regions are derived from US Geological Survey 1:24,000 topographic maps based on imagery dating to 1966 and provide a measure of relative glacier cover across the two states (Fountain et al. 2017).

Region	Number	Elevation[a] Max (m)	Min (m)	Mean (m)	Area Mean (km^2)	Median (km^2)	Total (km^2)
Oregon Cascades	48	3,415	1,342	2,392	0.67	0.38	31.71
California Cascades (Mt. Shasta)	6	4,266	2,998	3,549	0.81	0.97	4.85
Sierra Nevada	157	4,220	3,084	3,632	0.11	0.08	17.36
Klamath Range (Trinity Alps)	2	2,514	2,481	2,498	0.03	0.03	0.06

[a]Glacier elevation summaries derived from the mean elevation of individual glaciers.

increasing rate from the mid-1990s to the middle of the first decade of the 21st century, relative to an earlier period beginning in the 1950s to 1970s (Arendt et al. 2009). In southwestern Canada, glaciers have been retreating significantly since the 1950s (DeBeer and Sharp 2007, Bolch et al. 2010, Menounos et al. 2018). Similarly, in the western US exclusive of Alaska, glacier area has significantly decreased overall (Fountain et al. 2017), including the Wind River Range (DeVisser and Fountain 2015), the Lewis Range of Glacier National Park (Clark et al. 2017), the Olympic Mountains (Riedel et al. 2015), the North Cascades (Riedel and Larrabee 2016, Pelto 2018), and the Sierra Nevada (Basagic and Fountain 2011).

The glaciers of California are small, averaging 0.14 km^2 and covering 23.11 km^2 as of the 1980s (1 ha = 0.01 km^2) (Table 1; Fountain et al. 2017). They are found in three distinct regions: the Trinity Alps, Mt. Shasta, and the Sierra Nevada (Figure 1; Guyton 1998, Fountain et al. 2017). The largest glaciers flank Mt. Shasta, but the most extensive glacier cover occurs throughout the southern Sierra Nevada. The Trinity Alps have the least glacier cover and are among the smallest glaciers in California (Table 1). Glacier studies in California have largely focused on Mt. Shasta (Rhodes 1987, Howat et al. 2006) and the Sierra Nevada (Raub et al. 2006, Basagic and Fountain 2011, Moore and Moring 2013). While some glacier growth has been suggested for a couple of Mt. Shasta glaciers (Howat et al. 2006), later work has shown that the enlargement resulted from a kinematic wave, and despite the glacier advance the volume of the glaciers is shrinking (Andrew Fountain, Portland State University, unpublished data). Glaciers of the Trinity Alps are about 83 km southwest of Mt. Shasta, but differences in local climate and topography (Baker 1944, Sawyer 2006) and anomalous dynamic behavior of some Shasta glaciers make comparisons difficult.

The Trinity Alps glaciers represent the westernmost and lowest elevation modern ice in the conterminous US (Table 2) south of Olympic National Park, Washington (47° 34′N), providing a unique setting for examining glacier change relative to other Little Ice Age (LIA) glaciated regions. The purpose of our study was to inventory the glaciers in the Trinity Alps, define their changes since the end of the Little Ice Age in the late 19th century, and measure changes in two prominent perennial snowfields since the mid-20th century. Last, we examine climate over this period to help interpret the observed changes in the glaciers.

Study Area

The Trinity Alps are a subrange of the Klamath Mountains in California (Figure 1). The entire range is below 2,750 m elevation and is characterized by steep river canyons and rugged subalpine topography. Although the geology of the Klamath Mountains is complex, the study region is predominately granite dating to the Late Jurassic period when it intruded into the metamorphic host rock (Irwin 1966). The region was extensively eroded by dozens of cirque and valley glaciers up to 22 km long during the Pleistocene (Sharp 1960). The proximity to the Pacific Ocean, 89 km west,

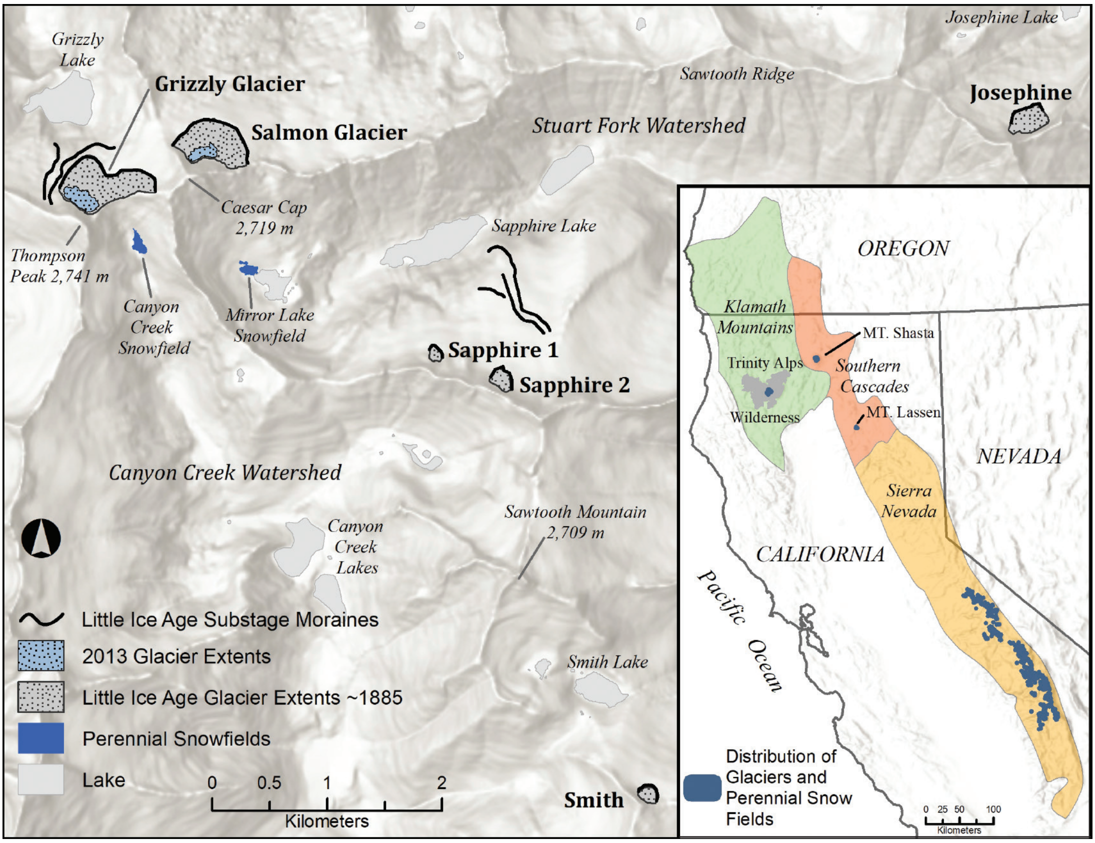

Figure 1. Map of the glacier and perennial snow regions of California with an expanded view of study area in the Trinity Alps Wilderness, Klamath Range, California. Six late 19th century (ca. 1885) glacier extents defined by conspicuous terminal moraines occur throughout the highest elevations of the Trinity Alps Wilderness. Two Little Ice Age (LIA) moraine sequences originally mapped by Sharp (1960), are shown in Stuart Fork (below Sapphire 1 and Sapphire 2) and Grizzly Creek watersheds indicating multiple LIA sub-stages. Two perennial snowfields are also identified in the Canyon Creek and Stuart Fork watersheds with outlines based on their 1955 extents. The region contains other less prominent perennial snowfields that were not a focus of our study.

creates a Mediterranean climate characterized by cool wet winters and warm dry summers with strong west to east gradients in precipitation and temperature (Sawyer 2006, Skinner et al. 2006). As with other small mountain glaciers in marginal climates for glaciers, those in the Trinity Alps persist due to favorable topographies that increase shading from tall headwalls and enhance localized snow accumulation through avalanching and wind transport (Kuhn 1995, Basagic and Fountain 2011). The glaciers of the Trinity Alps occur entirely below the tree line at an elevation of 2,460 m; far lower than other glaciated areas in California (Sharp 1960, Guyton 1998).

Previous Work

The presence of glaciers in the Trinity Alps was first mentioned by geologist Oscar Hershey who briefly stated “three tiny glaciers” occur in the “high-mountain cluster” east of Humboldt Bay (Hershey 1903). Hershey provided a location description for only one of the three glaciers as occurring “in a shadow of a high spur of Mt. Courtney.” Mt. Courtney is not recognized on United States Geological Survey (USGS) maps, but based on a detailed description of the area (see Hershey 1903), we conclude he was referring to Caribou Mountain (2,614 m) with the one glacier occurring below a high unnamed peak along Saw-

TABLE 2. Physical characteristics and status of six Little Ice Age (LIA) glaciers as defined by terminal moraines in the eastern portion of the Trinity Alps Wilderness, California.

Glacier	Lat	Long	Headwall height (m)	Aspect	Moraine elevation[a] (m)	Elevation range in 2013[b] (m)	ca. 1885 Area[c] (ha)	Status in 2009
Grizzly	41.003	–123.047	194	18°, NNE	2,347	2,466–2,588	24.44	Present
Salmon	41.006	–123.034	220	16°, NNE	2,394	2,450–2,536	19.40	Present
Josephine	41.008	–122.950	216	340°, NNW	2,156	NA	6.00	Extinct
Sapphire 1	40.990	–123.011	143	17°, NNE	2,285	NA	1.20	Extinct
Sapphire 2	40.988	–123.005	124	20°, NNE	2,306	NA	2.57	Extinct
Smith	40.955	–122.989	111	38°, NNE	2,346	NA	1.74	Extinct

[a]Elevation of the lowest point along the terminal moraine ridge.

[b]Estimated lower and upper glacier elevation extents in 2013.

[c]Estimated glacier size during the last glacial maxima (ca. 1885) based on the total area contained within the innermost terminal moraine ridge and its respective headwall; 1 hectare (ha) = 10,000 m^2.

tooth Ridge just south of Josephine Lake (Figure 1, Josephine Glacier).

The next known visit was fifty years later, when Robert Sharp from the California Institute of Technology studied the Pleistocene glaciation in the Trinity Alps. Sharp visited two glaciers in September of 1956; one (informally referred to as Grizzly Glacier) below Thompson Peak (2,742 m) in the headwaters of Grizzly Creek, North Fork Trinity River, and the other (informally referred to as Salmon Glacier) below Caesar Cap (2,720 m) in the headwaters of Thompson Creek, Southfork Salmon River, about 1 km east of Grizzly Glacier (Sharp 1960). Sharp mentioned the presence of crevasses at each glacier and a short distance beyond the ice margin were fresh boulder moraines. Although he did not measure the glaciers, Sharp estimated each covered 2.2 to 2.4 ha. Sharp did not locate the third glacier identified by Hershey (1903), but he suggested the most probable location might be above Lake Josephine (Sharp 1960).

Sharp did find evidence of a recently extinct glacier in the adjacent Stuart Fork drainage, above and southeast of Sapphire Lake, that could have been one of the three reported by Hershey (1903) (Figure 1). Sharp mapped a series of three similar "neoglacial moraines", hereafter LIA moraines, at the extinct Stuart Fork location and at Grizzly Glacier; Salmon Glacier has only one LIA moraine (Figure 1). Sharp (1960) described the innermost LIA moraines at Stuart Fork and Grizzly Glacier locations as "youthful and fresh" lacking significant vegetation, where the middle and outermost LIA moraines were "several times older" based on dense vegetative cover and the presence of mature conifer stands. The three moraines below Grizzly Glacier described by Sharp (1960), were dated to about 690, 150, and 130 years before 2013 (Graham 2013).

Meier's (1961) partial inventory of glaciers in the contiguous US identified Grizzly and Salmon glaciers from aerial photographs, estimating their elevations at 2,600 m and their total area to be 30 ha. This area is a gross overestimate, based on Sharp (1960) who visited the glaciers about the same time, and likely due to aerial photographs acquired during a period with extensive seasonal snow. Sawyer (2006) described visiting Grizzly and Salmon glaciers periodically over 40 years and reported substantial retreat during the drought of the late 1980s followed by purported glacier expansion in 1996. In the early 2000s, Heermance and Briggs (2005) estimated Grizzly and Salmon glaciers decreased in area by 10 to 20% over 50 years (1956 to 2005). Kavanaugh and Schoville (2009) visited Grizzly Glacier in 2008 and described the glacier as rapidly receding with large blocks of ice calving off the lower margins. Last, Fountain et al. (2014) estimated Grizzly and Salmon glaciers had lost 77 to 84% of their area from 1900 to 1993, assuming the moraines nearest the glacier were late LIA, about 100 years old.

Methods

Little Ice Age Glacier Inventory

The LIA glaciers in the Trinity Alps are poorly documented. Hershey (1903) recognized only three extant LIA glaciers despite the presence of multiple LIA moraines in the subalpine portion of the Trinity Alps (Sharp 1960). To inventory LIA glacier extents in the Trinity Alps, we identified all distinct LIA moraines using satellite imagery dated 26 July 2014 (Supplemental Table S1, available online) and handheld aerial photographs taken from low flying aircraft during October 2011 and September 2016. We limited our inventory to locations with clearly defined moraines occurring below smooth bedrock forelands. For each LIA glacier, we mapped glacier area (defined by the innermost moraine ridge and bottom of headwall) and measured topographic variables including headwall height, elevation at the lowest point along the terminal moraine ridge, and aspect using a 10-m digital elevation model (DEM). The satellite imagery was digitally examined in a geographic information system (GIS) (ArcGIS 10.3.1, ESRI Inc.) using the oblique handheld aerial photographs to aid interpretation. Because we only include locations with clearly defined moraines, our LIA inventory is conservative.

Long-Term Glacier and Perennial Snowfield Mapping

We used multiple characteristics from ground-based observations made during a low snow summer (2009) to define a glacier. We relied on observations of exposed ice, crevasses, and proximal moraines to define a perennial nature and movement (Cuffey and Paterson 2010). The Trinity Alps contain numerous seasonal snowfields, the extent of which is dependent on the previous winter's snowpack. Obtaining an inventory of perennial snowfield cover is more difficult than glaciers because identifying features requires extensive late-summer imagery for multiple years. We adopt the definition of perennial snow as features lacking glacial characteristics but occurring over multiple years with a standard deviation of late-summer area < 40% for > 20 years (DeVisser and Fountain 2015). Because suitable range-wide imagery is scarce, we examined specific snowfields through time rather than complete an entire inventory.

To quantify long-term changes in G&PS, we used LIA moraines, vertical aerial orthophotos, high-resolution satellite images, and field mapping with a geographic positioning system (GPS) (Supplemental Table S1). We restricted available imagery to years having minimal residual snow cover in late summer. We did not use G&PS outlines available from the USGS (1:24,000) topographic maps as a data source because the original aerial photography used to make the maps exhibited extensive residual snow cover (Fountain et al. 2007). Also, LandSat imagery was omitted because the spatial resolution (15 m) was too coarse for our analysis given the small size of G&PS in the Klamath Mountains (Krimmel et al. 2002).

We obtained nine aerial and satellite images acquired from 1955 to 2015 (Supplemental Table S1). All aerial photographs had spatial resolutions of 1 m; satellite imagery resolutions ranged from 0.33 to 0.5 m. All images were rectified and georeferenced products except for the 1972 aerial photographs, which were rectified using six ground-based control points including small ponds, boulders, moraine ridges, and geologic dikes identified on the digital orthophoto quadrangle imagery (acquired July 2014), prior to mapping glacier areas (Basagic and Fountain 2011, DeVisser and Fountain 2015). In addition, we mapped the glacier perimeter using a GPS with an accuracy ± 2.6 m.

We manually digitized all G&PS outlines from the imagery at a scale of 1:700 in a GIS. All mapped perimeters were identified by two independent observers. This allowed for potential mapping errors or feature interpretation discrepancies to be resolved through consensus. Last, we established ground-based photograph monitoring stations at each of the two glaciers to document qualitative changes in glacier geometry and morphology during field visits between the years of 2009 and 2018.

Uncertainty

Uncertainty evaluation follows DeVisser and Fountain (2015), who identify three sources of potential error from maps or orthorectified aerial photographs. Positional uncertainty (U_p) is the uncertainty caused by distortion in the base image or map from the orthorectification process. Digitizing uncertainty (U_d) is determined by measuring how well a digitized outline follows the actual perimeter. Finally, interpretation uncertainty (U_i) is the questionable location of the G&PS margin due to rock debris or shadows obscuring margins, or by seasonal snow cover obscuring the margin of glaciers. The total uncertainty (U_t) for each feature is the square root of the sum of the square of each contributing uncertainty (Baird 1962).

$$U_t = \sqrt{U_p^2 + U_d^2 + U_i^2} \qquad \text{(Eqn 1)}$$

To evaluate Eqn1, we ignored positional uncertainty (U_p) for georeferenced digital orthophoto quadrangles (DOQs) because we were concerned with area not exact location. Furthermore, the digitized points are highly correlated such that they are not independently determined. However, to make use of an unorthorectified aerial photo from 1972 we calculated values for U_p to account for remaining uncertainty after the georeferencing process. We defined U_p for the 1972 photographs by determining the root mean squared error (RMSE) difference in distance between six control points used at each of the two glaciers from the 26 July 2014 DOQ and the 1972 aerial image. To evaluate the digitizing uncertainty, we followed Hoffman et al. (2007) who adapted the method of Ghilani (2000). This uncertainty is a product of the length of the side of a square (S) that has the same area as the feature polygon in question multiplied by the RMSE linear uncertainty (σ_d),

$$U_d = S\sigma_d\sqrt{2} \qquad \text{(Eqn 2)}$$

This method assumes vertices are well correlated and is independent from the number of vertices a feature may contain. Our study includes four relatively small G&PS features with high quality imagery (i.e., ≤ 1 m raster pixel resolution) which allowed us to confidently digitize feature perimeters. To evaluate the digitizing uncertainty (U_d) we used Eqn 2 with the image raster pixel resolution as the linear uncertainty (σ_d) in the DOQs and aerial photos. To define U_d for the GPS track we used the estimated accuracy of ± 2.6 m at the time of mapping as the linear uncertainty (σ_d) (Eqn 2). Last, interpretation uncertainty (U_i) was estimated only for glaciers because the two perennial snowfields in the study lacked any visual obstructions obscuring the margins such as shadows or rock debris. The cases where glacier margins were visually obscured were exclusively caused by residual snow cover in the 1955 and 1972 images. To estimate interpretation uncertainty in these examples, we outlined each glacier extent twice. The first outline included only clean and debris-covered ice as indicated by crevasses. The second outline included the uncertain shadowed ice/snow and the debris-covered or snow-covered glacier ice. The U_i was then determined as one-half of the difference between the two areas outlined.

Climate Trend Analysis

To examine the response of G&PS in the Trinity Alps to variations in climate, we compared changes in glacier area to winter precipitation and summer air temperature from the PRISM re-analysis data (Daly et al. 2008, PRISM Climate Group 2018), employing a similar analysis as Sitts et al. (2010), using data for the 4 km × 4 km PRISM grid cell centered on Thompson Peak (Figure 1) for the period of January 1895 to September 2015. We calculated total winter precipitation (December to February) as the sum of monthly totals to characterize annual snow accumulation. This period has the greatest snow accumulation and excludes the transition months of November and March in which precipitation is more likely to fall as rain. To characterize summer ablation, we calculated mean summer temperatures from the warmest three months of the year (July through September). Three-year backward running means (average three years and dating the result for the youngest year) were applied to winter precipitation and summer temperatures (Nye 1960, Jóhannesson et al. 1989, Raper and Braithwaite 2009). Lastly, we calculated standardized residuals of the three-year backward running means by subtracting the long-term mean and dividing by the standard deviation.

Results

Observed moraines suggest at least six LIA glaciers existed in the Trinity Alps during the latest LIA glacial advance (Table 2, Figure 1). Graham (2013) estimated the last glacial contact with the inner-most Grizzly Glacier moraine at about 1885 using ^{10}Be cosmogenic dating and dendrochronology corrected for ecesis. The morphology and scale of this LIA moraine is nearly identical to the moraine nearest Salmon Glacier occurring < 1 km east. In addition, the four other smaller moraines we identified in the region occurred at similar elevations and shared similar physical settings that promote snow accumulation and topographic shading from northern aspects and steep headwalls (Table 2, Figure 1). Given these similarities, we assume all LIA glaciers were in contact with moraines around 1885. The total 1885 LIA glacier area among the six glaciers was 55.4 ha (Table 2), with individual features ranging in size from 1.2 ha to 24.4 ha (Table 2).

Glacier Area

At the start of our field work in 2009 only two glaciers remained, Grizzly and Salmon. Both exhibited exposed ice, crevasses, dry calving, and basal slippage—found during inspections underneath crevasse openings. Grizzly Glacier also maintained a prominent bergshrund crevasse near the top of the accumulation zone. Most imagery provided clear feature definition making perimeter mapping straightforward. However, in September 2009, only 63% of Grizzly Glacier perimeter was field mapped because of safety concerns along the headwall. To complete the perimeter mapping along the headwall, the June 2009 DOQ was used. We believe little error was added because the headwall is a near-vertical rock cliff and the upper glacier margin changes little from June to September. Salmon Glacier was not field-mapped at this time due to unsafe calving conditions. Also, the September 2014 satellite image was stretched (i.e., distorted) over Salmon and Grizzly glacier headwalls obscuring their upper margins. To complete mapping of the upper margin for September of 2014, a high-quality DOQ from July 2014 was used as glacier margins were completely exposed due to a record low snowpack of 9% of the 01 April average from the winter of 2013 to 2014 (California Department of Water Resources 2018).

Changes in area for Grizzly and Salmon glaciers since ca. 1885 have been extensive. The total area of Grizzly and Salmon glaciers decreased by 31.38 ± 1.25 ha (72%, –1% yr^{-1}) from ca. 1885 to 1955 when the first reliable imagery became available (Table 3, Figure 2). By 1972 the total glacier area decreased another 2% (–0.1% yr^{-1}) of the ca. 1885 area to 11.58 ± 0.72 ha. By 1994 glacier area declined another 6% (–0.3% yr^{-1}) to 9.14 ± 0.04 ha. By 2013, the glaciers lost another 7% (–0.8% yr^{-1}) of the ca. 1885 area to 5.99 ± 0.03 ha. Between 1994 and 2013, Salmon Glacier experienced far greater fractional losses relative to the 1994 area (53%) than Grizzly Glacier (16%) (Figure 3). This difference in shrinkage rate between the two glaciers was not present in earlier periods of measurement and only accelerated since 1994 (Table 2, Figure 3). For example, between July and October 2014, Salmon Glacier lost 65% of its July area whereas Grizzly Glacier lost only 27% of its July area (Table 3).

Between 2013 and 2015 total glacier area decreased substantially from 5.99 ± 0.03 ha to 1.67 ± 0.01 ha representing a 72% decline since 2013 and the extinction of Salmon Glacier. During the summers of 2013 and 2014 Salmon Glacier experienced substantial calving, and by the end of 2014 it had stagnated. By fall of 2015 Salmon Glacier completely melted away (Figure 4). In 2015, the lower 54% of Grizzly Glacier broke apart into hundreds of large ice blocks leaving only the upper portion of the glacier intact (Figure 5). We visually approximated the ice blocks to be 2 to 8 meters across, with larger blocks occurring at higher elevations near the remaining intact portion of the glacier (Figure 5). Three and four years later, in September of 2018 (Figure 5) and 2019, Grizzly Glacier was covered in considerable snow and firn. Further inspection of the

TABLE 3. Estimated areas in hectares (1 hectare [ha] = 10,000 m^2) and percent of area uncertainties (%U) of Grizzly and Salmon glaciers and the Canyon Creek and Mirror Lake perennial snowfields from ca. 1885 to 2015, Trinity Alps Wilderness, California. NM = not measured.

	Glacier Area (ha)				Perennial Snowfield Area (ha)			
Year	Grizzly	%U	Salmon	%U	Canyon Creek	%U	Mirror Lake	%U
ca. 1885	24.44	0.20	19.40	0.22	NM	NM	NM	NM
1955	6.01*	5.16	6.45*	14.51	1.57	0.79	1.45	0.82
1972 (Aug)	6.00*	5.28	5.58*	8.54	1.29	0.87	1.07	0.95
1994 (Aug)	4.60	0.46	4.54	0.46	0.79	1.11	0.62	1.26
2009 (Sept)	3.96	1.43	NM	NM	NM	NM	NM	NM
2013 (Oct)	3.85	0.50	2.14	0.68	0.74	1.15	0.08	3.53
2014 (July)	3.59	0.52	1.85	0.73	0.24	2.00	0.00	0.00
2014 (Sept)	2.99	0.41	1.09	0.68	0.06	3.00	0.00	0.00
2014 (Oct)	2.62	0.29	0.65	0.58	0.00	0.00	0.00	0.00
2015 (Oct)	1.67	0.55	0.00	0.00	0.00	0.00	0.00	0.00

* Estimated average areas are presented due to residual snow cover partially obscuring lower glacier margin; see methods section for specific details.

glacier indicated it was thickening and advancing downslope into the stagnation zone of 2015 based on newly formed crevasses and basal slippage. During our inspections in September 2018 and 2019, the site of Salmon Glacier also accumulated substantial firn and snowpack since the glacier melted away in 2015.

Loss of Perennial Snowfields

Analysis of aerial imagery starting in 1955 revealed two features in the Trinity Alps Wilderness that met our definition of perennial snow and dated to at least 1955 when the first imagery was available. One perennial snowfield was located at the head of the Stuart Fork drainage above Mirror Lake at the base of the headwall (Figure 1, Mirror Lake Snowfield). The other snowfield was located over the ridge to the west at the head of adjacent Canyon Creek basin, also at the base of a headwall (Figure 1, Canyon Creek Snowfield). The combined area of the two features was 3.02 ± 0.02 ha in 1955, 2.36 ± 0.02 ha in 1972, and 1.41 ± 0.02 ha in 1994 (Table 3). By July of 2014 the Mirror Lake snowfield had ablated away (Table 3, Figure 3). The Canyon Creek snowfield disappeared shortly after in October of 2014 (Table 3). Other snowfields within the Trinity Alps likely met our definition as perennial but available range-wide imagery was too sparse to conduct a long-term analysis. Based on a review of the aerial and satellite imagery and field visits, all perennial snowfields throughout the Trinity Alps and greater Klamath Mountains of southern Oregon and northern California had fully ablated by 2014.

Glacier and Perennial Snowfields and Climate Trends

The climatological record in the Trinity Alps, since 1895, is characterized by a combination of decadal-scale patterns and shorter periods of high variability. Negative summer temperature anomalies persisted for nearly 30 years (1908 to 1937), followed by a period of nearly half a century (1938 to 1987) in which positive or negative temperature anomalies persisted for between 2 and 12 years (Figure 6). Summer temperatures have been above average every year since 2001 and have exceeded one standard deviation above the 1895 to 2015 average in 10 of the past 15 years (2001 to 2015) (Figure 7). Winter precipitation demonstrated higher frequency variability as compared to summer temperatures, with shorter periods of persistent positive or negative anomalies. Multi-year periods of low precipitation occurred in the Trinity Alps from approximately 1915 to the late 1930's, most of the 1940's, most of the 1960's, and from the mid-1980's to mid-1990's. Coincident with the California drought (Ullrich et al. 2018), winter precipitation in the Trinity Alps was below average from 2012 to 2016.

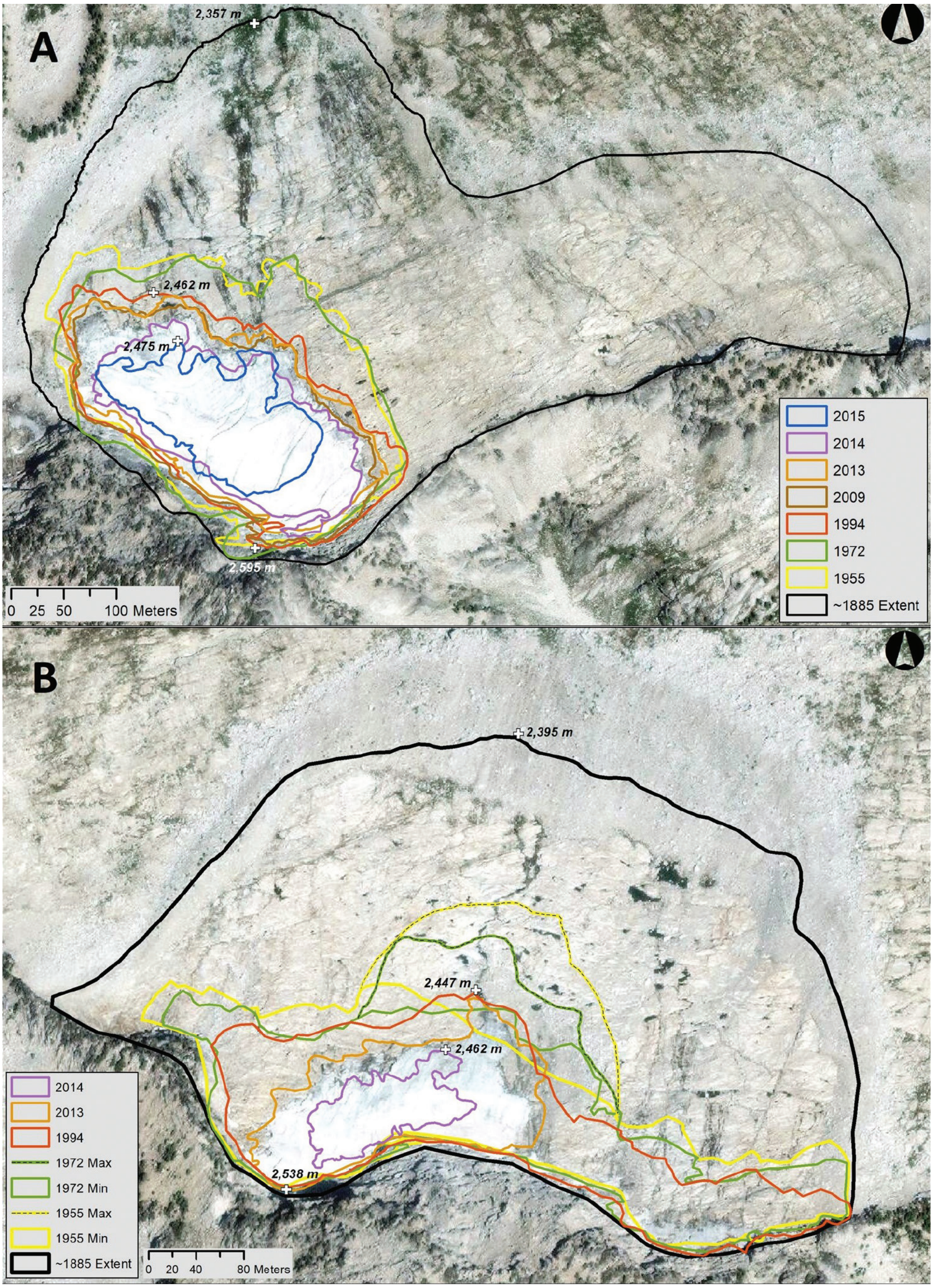

Figure 2. Digitized outlines of Salmon Glacier (A) and Grizzly Glacier (B) from approximately 1885 to 2015 in the Trinity Alps Wilderness, California. Salmon Glacier disappeared completely by the fall of 2015. The 1885 outlines were generated by mapping the ridgelines of prominent Holocene moraines coupled with mapping the near vertical bedrock headwalls at the upper extent of the glaciers. The 1885 outlines represent the most recent Little Ice Age (LIA) glacial advance. Due to extensive residual snow cover on Salmon Glacier in 1955 and 1972, outlines include a minimum estimated area (solid colors) and additional maximum estimated area dotted lines. Satellite base image date is from 26 July 2014. Approximate surface elevations are noted at four locations at each glacier.

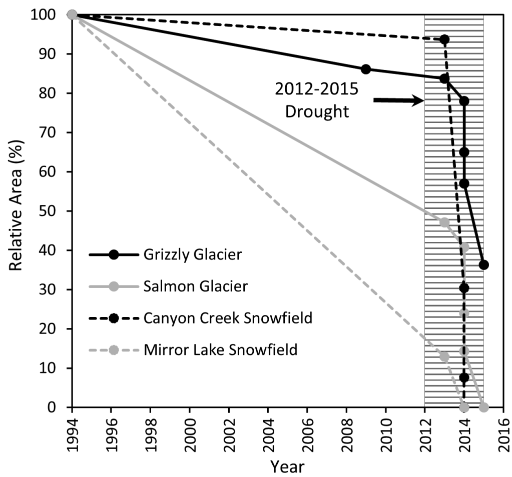

Figure 3. Changes in relative area for glaciers and perennial snowfields from 1994 to 2015, Trinity Alps Wilderness, California.

Discussion

Little Ice Age Glaciers

Prior to this study, only three LIA glacial features were noted in the greater Klamath Mountains. Based on the presence of conspicuous young moraines, we documented six small LIA glaciers among the highest elevations of the Trinity Alps portion of the Klamath Range. Because our analysis was largely restricted to remote sensing, there may be other less visible LIA moraines in the region. Only the largest two of the six LIA glaciers were present at the start of our study indicating the regional climate has changed over the past 100 years resulting in glacier loss similar to other regions worldwide (IPCC 2013, Zemp et al. 2015). The four locations where glaciers disappeared either occurred at lower elevations or had shorter headwalls than the two remaining glaciers, resulting in these locations having less snow accumulation and less topographic shading (Kuhn 1995). The series of three LIA moraines mapped by Sharp (1960) at two of the six locations in this study indicate multiple distinct glacier advances have occurred in the region during the LIA. Graham (2013) estimated the three LIA moraine ages below Grizzly Glacier and found the oldest to be around 700 years ago (ca. 1300) and the most recent about 130 years ago (ca. 1885) indicating a complex climate history in recent centuries. Little Ice Age glacier chronologies have also been described in the Sierra Nevada (Matthes 1940, Gillespie and Zehfuss 2004, Bowerman and Clark 2011) and Cascades (Osborn et al. 2012). However, differences in the estimated chronologies (Solomina et al. 2016) often with large variation around dating estimates, limit the ability to determine if any synchronous glacier responses to climate patterns among the three mountain ranges existed during the LIA.

Changes in Modern Glaciers and Perennial Snowfields

The magnitude of area change for the two Trinity Alps glaciers equaled –79% from ca.1885 to 1994, and –97% by the fall of 2015 with the complete loss of Salmon Glacier. This fractional area loss is much greater than observed in other glaciated regions of the western United States and Canada, including glaciers of California's Sierra Nevada (–55%, 1903 to 2004) (Basagic and Fountain 2011); the Cascade Range (OR and WA) including Mount Hood (–34%, 1901 to 2004) (Jackson and Fountain 2007), Mount Adams (–49%, 1904 to 2006) (Sitts et al. 2010), and Mount Rainier (–19%, 1910 to 1994) (Nylen 2004); the Olympic Peninsula in Washington (–34%, 1980 to 2009) (Riedel et al. 2015); the Colorado Front Range (–40%, 1909 to 2004) (Hoffman et al. 2007); the Wind River Range in Wyoming (–47%, 1900 to 2006) (Devisser and Fountain 2015); and the Canadian Rocky Mountains (–15%, 1952 to 2001) (Debeer and Sharp 2007). A broader study by Fountain et al. (2017) estimated a 39% decrease in glacier area throughout all glaciated regions of the American west between 1955 and 1990. These regional and continental changes reflect the decline of glaciers throughout the world (Zemp et al. 2019).

The pattern of change in the glaciers of the Trinity Alps over the last century—rapid loss in the early 20th century, followed by a slow retreat mid-century, and an acceleration in retreat by 2009 follows the general pattern in this region. In the early part of the 20th century glaciers retreated

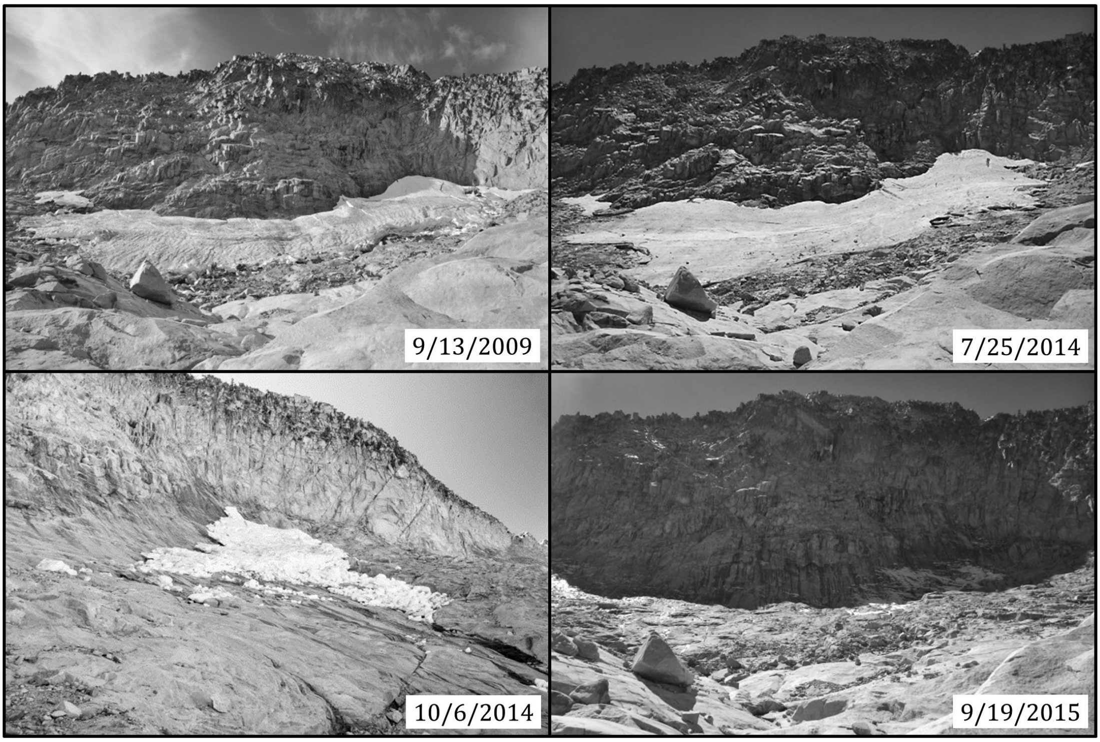

Figure 4. Repeat oblique photographs of Salmon Glacier taken by J. Garwood (13 September 2009 and 19 September 2015), R. Bourque (25 July 2014), and J. Barnes (06 October 2014) within the feature's Little Ice Age (LIA) moraine, Trinity Alps Wilderness, California. The 06 October 2014 image was taken northeast of the feature facing southwest whereas the others were taken north of the feature facing due south. The glacier broke apart (i.e., stagnation) in 2014 and completely melted away by the fall of 2015. The patchy snow observed in shadows of the 2015 image accumulated during a small storm that occurred two days prior to the image date. Photo Station Coordinates: lat 41.007734, long –123.032998.

rapidly in the western US in response to the end of the Little Ice Age and warming of air temperatures (Basagic and Fountain 2011, DeVisser and Fountain 2015, Hoffman et al. 2007). The slowing of the retreat, and slight advance of some glaciers in mid-20th century, is a result of the well-recognized mid-century cool period (Hubley 1956, Conway et al. 1999, Thompson et al. 2010). Subsequent glacier retreat generally resumed by the 1990s (Basagic and Fountain 2011, O'Neel et al. 2019), but for unknown reasons was delayed in the Trinity Alps until around 2009.

The reason for the more rapid retreat of Salmon Glacier compared to the Grizzly Glacier is not clear. We suspect it is due to the combination of small influences. The maximum elevation of Salmon Glacier was about 52 m lower than Grizzly in 2013 (Table 2) implying warmer air temperatures. The recent orientation of Salmon Glacier was NNW compared to the NE-facing Grizzly Glacier (Figure 2), thus exposing it to more solar radiation in the afternoon when air temperatures are the warmest. Both glaciers faced NNE (18°, 16°, respectively) in ca. 1885 but since that time they retreated into terrain with different aspects. Finally, the subglacial topography of Grizzly Glacier, based on exposed bedrock slope, appears to be concave compared to the relatively uniform bed slope of Salmon implying that Grizzly Glacier may be thicker and therefore would retreat less quickly than Salmon Glacier. Perhaps these small differences would not be significant for a pair of relatively large glaciers, but for Salmon and

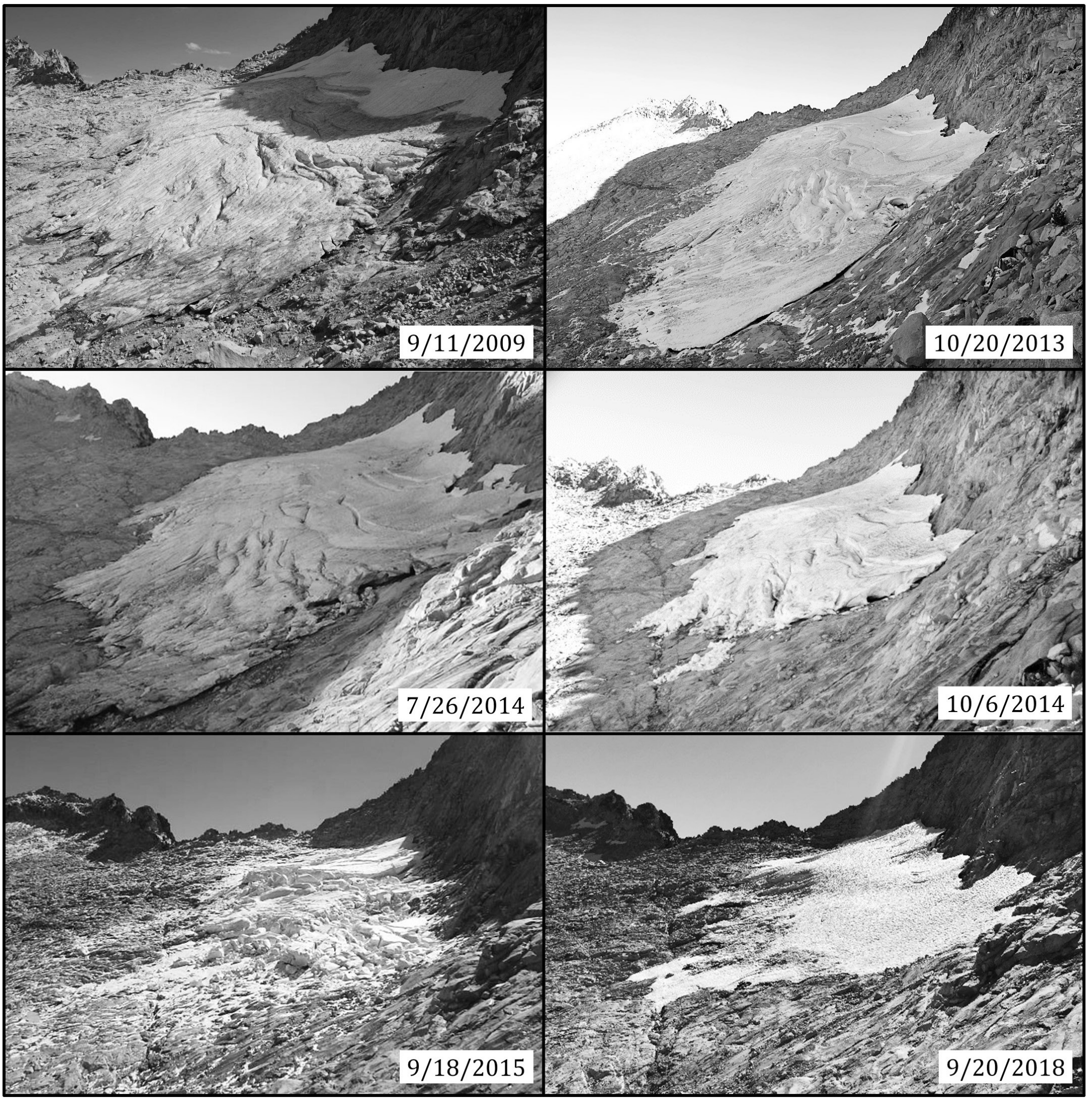

Figure 5. Repeat oblique photographs of Grizzly Glacier taken from the top of the western Holocene moraine, Trinity Alps Wilderness, California. The lower half of the glacier broke apart in the fall of 2015. A thin layer of fresh snow visible in the 18 September 2015 image accumulated during a brief storm that occurred two days prior to the image date. This snow cover visually exaggerates the actual glacier size beyond the visible pile of scattered ice debris visible in the photo; a result of extreme calving in the lower half of the feature during the summer of 2015. All photographs taken by J. Garwood with exception of 20 October 2013 by K. Lindke and 06 October 2014 by J. Barnes. Photo Station Coordinates: lat 41.00321, long –123.05064.

Grizzly that have been on the edge of existence, these differences may be important.

The persistence of glaciers in the Trinity Alps over the past century has been remarkable given their low elevation and low latitude; and attests to the importance of local factors favoring glacier survival (Kuhn 1995). This region hosts the lowest elevation ice in California (between 2,447 and 2,595 m above sea level), more than 500 m lower than the glaciers on Mt. Shasta and 600 m lower than those in the Sierra Nevada (Fountain et al. 2017). We suggest that the glacier location at the bottom of northeast-facing headwall cliffs below the two highest summits in the Trinity Alps is the

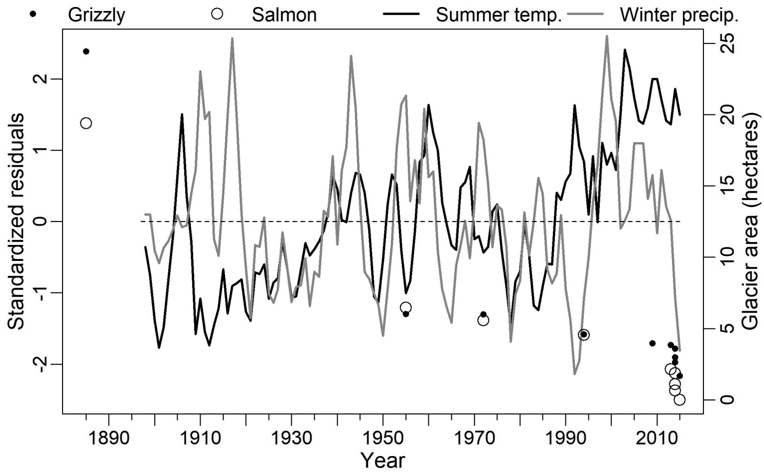

Figure 6. Three-year backward running standardized residuals of means of winter (Dec to Feb) precipitation and summer (Jul to Sep) temperature from 1895 to 2015, and measured glacier areas for Grizzly and Salmon glaciers from ca. 1885 to 2015, Trinity Alps Wilderness, California. Winters are dated for the calendar year in which the winter ended. Temperature and precipitation data are from a reanalysis product (Daly et al. 2008). Standardized residuals were calculated as the observed value, minus the 1895 to 2015 average, divided by the standard deviation.

primary reason for their existence. The headwalls provide protection from solar radiation and avalanching provides additional snow accumulation. Wind deposition may also play a role. The record of glacier and perennial snow responses to local climate patterns in this unusual topo-climactic setting provides an important comparison to other glacier populated regions.

Although large data gaps exist, clearly the largest magnitude of ice loss in the Trinity Alps since the end of LIA occurred during the first half of the 20th century. Since then, the glaciers have receded at a much slower but steady rate until the most severe California drought years of 2013 to 2015. The modern drought differs from earlier periods of persistent low precipitation by coinciding with a period of consistent record-high summer temperatures (Ullrich et al. 2018) (Figure 6). Warm summer temperatures have been recognized as a major contributor to the severity of the extended 2012 to 2016 California drought, increasing the severity by as much as 36% (Griffin and Anchukaitis 2014, Williams et al. 2015, Ullrich et al. 2018). Three-year backward running mean summer temperatures in the Trinity Alps during the drought ranged from 1.37 (in 2013) to 1.86 (in 2014) standard deviations above the long-term average (Figure 6). In addition, winter and spring temperatures are increasing across North America resulting in less snowpack in spring and early summer (Mote et al. 2005, Westerling et al. 2006, Shukla et al. 2015, Luo et al. 2017, Mote et al. 2018).

In the second half of the 20th century, the Klamath Mountains have seen some of the largest reductions in measured 01 April snow water equivalent in the Western United States (Mote et al. 2005, Mote et al. 2018). The lack of winter precipitation in the Klamath Mountains during the California drought was rare but not unprecedented in the long-term record; 01 April snowpack was below normal from 2012 to 2015 with a steady decrease through time: 2012 (94%), 2013 (43%), 2014 (9%), and 2015 (3%) (California Department of Water Resources 2018). But unlike precipitation, snowpack during the drought (particularly in 2014 and 2015), was unmatched since 1950. No other year since 1950 had an 01 April snowpack less than 34 percent in the Klamath Mountains (California Department of Water Resources 2018). Because the drought years of 2013 to 2015 were so severe, residual snow disappeared during the early part of the summer (May to July). For example, the Canyon Creek snowfield shrunk in area by 68% from 10 October 2013 to 26 July 2014, a period that normally experiences snow accumulation prior to summer snowmelt (Figure 6). In 2014 and 2015, Salmon and Grizzly glaciers started the ablation season with little to no snow cover.

Howat et al. (2006) suggested that changes in glacial extent on Mt. Shasta were primarily driven by winter precipitation rather than summer temperatures. We find that substantial decreases in glacial area, and the extinction of one glacier, occurred during a period of low, but not unprecedented winter precipitation while summer temperatures were at unprecedented highs. Winter precipitation has been below the long-term average (1895 to 2015) in nine of the past 20 years (1996 to 2015; Figure 7) in the Trinity Alps, whereas summer temperatures have exceeded the long-term average in 18 of the past 20 years. Precipitation deficits equivalent to, or more severe than, those experienced from 2013 to 2015 have occurred in the Trinity Alps in the past century (Figure 6), but none have occurred when summer temperatures have remained consistently well above the long-term average. While we have not formally quantified change in glacial area as a function of winter precipitation and summer temperatures, it seems evident that glacial retreat in the Trinity Alps is largely attributable to unprecedented and consistently high summer temperatures. It also seems likely that the observed extinction of Salmon Glacier is the first time this has occurred after the end of LIA around 1885, given that the area of Salmon Glacier remained relatively stable during earlier periods of persistent low precipitation (e.g., 1960s, and mid-1980s to mid-1990s), when summer temperatures were less extreme.

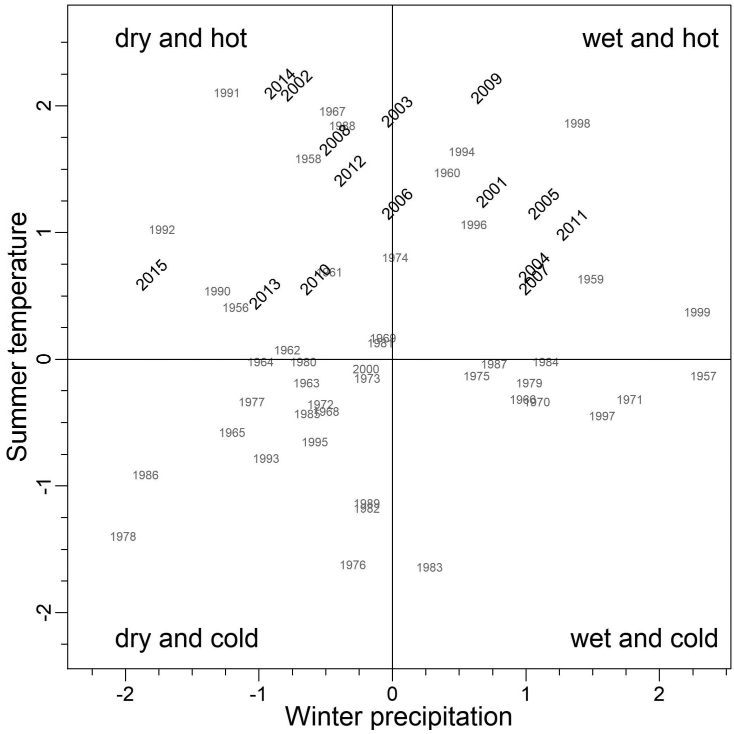

Figure 7. Standardized residuals of annual winter (Dec to Feb) precipitation and summer (Jul to Sep) temperature from 1955 to 2015, Trinity Alps Wilderness, California. Winters are dated for the calendar year in which the winter ended. Data are from a reanalysis product (Daly et al. 2008). For reference, 1955 represents the first aerial image we had available to measure glacier and perennial snowfield areas. Years presented in black represent the most recent 15 years of this study (2001 to 2015).

Glacier and Perennial Snowfield Dependent Ecosystems

The Klamath Range is globally recognized for its rich temperate biodiversity (DellaSala et al. 1999, Olson et al. 2012). Modern glaciers and perennial snowfields are rare in this region compared to other glaciated ranges throughout the western US. However, glacial ice and persistent snow influence local biodiversity and species distributions by extending perennial wetlands into high elevations normally lacking surface waters. For example, Kavanaugh and Schoville (2009) described a new species of beetle (*Nebria praedicta*) currently endemic only to Grizzly Glacier. Like other examples from the *Nebria* genus, this species depends on perennial snow and ice as a fundamental niche to maintain the cool microclimate needed to survive (Kavanaugh and Schoville 2009). In addition, Schoville and Graening (2013) documented two species of ice-crawlers on the margins of Grizzly Glacier: *Grylloblatta marmoreus* and another *Grylloblatta* sp. awaiting formal description. Like

Nebria beetles, these insects depend on cold microclimates and current distribution estimates for each species are ≤ 1 km^2 (Schoville and Graening 2013). The coastal tailed frog (*Ascaphus truei*), a California Species of Special Concern (Thomson et al. 2016), is adapted to perennial cold-water streams and its current range-wide elevation record was discovered in 2009 at 2,203 m (Garwood, unpublished data), directly below the Canyon Creek snowfield, which disappeared in the fall of 2014. Lastly, three of the four watersheds in this study contribute glacial and/or snowmelt driven cold-water streamflow directly to anadromous fish-bearing streams containing spring Chinook salmon (*Oncorhynchus tshawytscha*) and summer steelhead (*Oncorhynchus mykiss*) populations—both currently being considered for listing under the Federal Endangered Species Act (Federal Register 2018, 2019). These salmonids migrate annually from the Pacific Ocean to these streams during spring and stage in deep cold-water pools throughout the summer months before spawning in the fall (Nakamoto 1994, Moyle 2002). Given the dramatic local declines of glacial ice and persistent autumn snow in the Klamath Range (Mote et al. 2018), climate change threatens the unique distributions and resiliency of these stenothermic fauna adapted to local glacier and snow dependent environments, including the persistence of the newly discovered beetle, *Nebria praedicta*.

Acknowledgments

Many thanks to Tony LaBanca, Gordon Leppig, Daniel Barton, Jason Barnes, Ryan Bourque, and Melissa Reneski for assisting the project on various field visits. This work was supported by a grant from California Association of Professional Scientists to MvH for purchasing critical satellite imagery used in our analysis. Thanks to Curt Babcock and the California Department of Fish and Wildlife for covering publication fees. Jason Barnes provided early GIS support and helped obtain some imagery used in our analysis. Ken DeCamp shared historic and contemporary oblique photographs that aided in mapping interpretations. We also thank our partners, Rebecca Garwood, Christine van Hattem, and Melissa Reneski for supporting our frequent excursions into the backcountry. The US Geological Survey via the Western Mountain Initiative funded co-author Andrew Fountain's participation in this study. This manuscript was improved by comments from Robin Lesher, Dylan Fischer, and two anonymous reviewers.

Literature Cited

Ahlmann, H. W. 1953. Glacier variations and climatic fluctuations. Bowman Memorial Lectures, Series 3. American Geographical Society, New York, NY.

Arendt, A., J. Walsh, and W. Harrison. 2009. Changes of glaciers and climate in northwestern North America during the late twentieth century. Journal of Climate 22:4117-4134.

Baird, D. C. 1962. Experimentation: An Introduction to Measurement Theory and Experiment Design. Prentice Hall, Englewood Cliffs, NJ.

Baker, F. 1944. Mountain climates of the western United States. Ecological Monographs 14:223-254.

Basagic, H. J., and A. G. Fountain. 2011. Quantifying 20th Century glacier change in the Sierra Nevada, California. Arctic, Antarctic, and Alpine Research 43:317-330.

Bolch, T., B. Menounos, and R. Wheate. 2010. Landsat-based inventory of glaciers in western Canada, 1985–2005. Remote Sensing of Environment 114:127-137.

Bowerman, N. D., and D. H. Clark. 2011. Holocene glaciation of the central Sierra Nevada, California. Quaternary Science Reviews 30:1067-1085.

Brown, L. E., D. M. Hannah, and A. M. Milner. 2007. Vulnerability of alpine stream biodiversity to shrinking glaciers and snowpacks. Global Change Biology 13:958-966.

California Department of Water Resources. 2018. California Data Exchange Center, Snow Course Measurements. Available at: http://cdec.water.ca.gov/reportapp/javareports?name=COURSES (accessed 5 November 2018).

Clark, A., D. Farge, E. Peitzsch, B. Reardon, and J. Harper. 2017. Glaciological measurements and mass balances from Sperry Glacier, Montana, USA, years 2005–2015. Earth System Science Data 9:47-61.

Conway, H., L. A. Rasmussen, and H. P. Marshall. 1999. Annual mass balance of Blue Glacier, USA: 1955–97: Geografiska Annaler: Series A. Physical Geography 81:509-520.

Cuffey, K. M., and W. S. B. Paterson. 2010. The Physics of Glaciers. Academic Press, Amsterdam.

Daly, C., M. Halbleib, J. Smith, W. Gibson, M. Doggett, G. Taylor, J. Curtis, and P. Pasteris. 2008. Physiographically-sensitive mapping of temperature and precipitation across the conterminous United States. International Journal of Climatology 28:2031-2064.

DeBeer, C. M., and M. J. Sharp. 2007. Recent changes in glacier area and volume within the southern Canadian Cordillera. Annals of Glaciology 46:215-221.

DellaSala, D. A., S. B. Reid, T. J. Frest, J. R. Strittholt, and D. M. Olson. 1999. A global perspective on the biodiversity of the Klamath-Siskiyou ecoregion. Natural Areas Journal 19:300-319.

DeVisser, M. H., and A. G. Fountain. 2015. A century of glacier change in the Wind River Range, WY. Geomorphology 232:103-116.

Federal Register. 2018. Endangered and threatened wildlife; 90-day finding on a petition to list Chinook salmon in the upper Klamath-Trinity Rivers Basin as threatened or endangered under the Endangered Species Act. Federal Register 83:8410-8414, Washington, DC.

Federal Register. 2019. Endangered and threatened wildlife; 90-day finding on a petition to list summer-run steelhead in northern California as threatened or endangered under the Endangered Species Act. Federal Register 84:16632-16636, Washington, DC.

Fountain, A. G., H. J. Basagic IV, C. Cannon, M. DeVisser, M. J. Hoffman, J. S. Kargel, G. J. Leonard, K. Thorneykroft, and S. Wilson. 2014. Glaciers and perennial snowfields of the US Cordillera. *In* J. Kargel, G. Leonard, M. Bishop, A. Kääb, and B. Raup (editors), Global Land Ice Measurements from Space, Springer Praxis Books, Springer, Berlin, Heidelberg. Pp. 385-408.

Fountain, A. G., B. Glenn, and H. J. Basagic. 2017. The geography of glaciers and perennial snowfields in the American West. Arctic, Antarctic, and Alpine Research 49:391-410.

Fountain, A. G., M. J. Hoffman, K. Jackson, H. J. Basagic, T. H. Nylen, and D. Percy. 2007. Digital outlines and the topography of the glaciers of the American West. US Geological Survey Open-File Report 2006-1340.

Fountain, A. G., and W. V. Tangborn. 1985. The effect of glaciers on streamflow variations. Water Resources Research 21:579-586.

Frans, C., E. Istanbulluoglu, D. P. Lettenmaier, A. G. Fountain, and J. Riedel. 2018. Glacier Recession and the Response of Summer Streamflow in the Pacific Northwest United States, 1960–2099: Water Resources Research 54:6202-6225.

Gillespie, A. R., and P. H. Zehfuss. 2004. Glaciations of the Sierra Nevada, California, USA, Quaternary Glaciations—Extent and Chronology, Part II. 51-62. Elsevier, Amsterdam.

Ghilani, C. D. 2000. Demystifying area uncertainty: more or less. Surveying and Land Information Systems 60:177-182.

Graham, J. T. 2013. Late Holocene glacial advances in the Klamath Mountains, northern California, determined from ^{10}Be cosmogenic exposure dating and dendrochronology. M.S. Thesis, California State University, Northridge.

Griffin, D., and K. J. Anchukaitis. 2014. How unusual is the 2012–2014 California drought? Geophysical Research Letters 41:9017-9023.

Guyton, B. 1998. Glaciers of California. University of California Press, Berkeley.

Hall, M. H., and D. B. Fagre. 2003. Modeled climate-induced glacier change in Glacier National Park, 1850–2100. BioScience 53:131-140.

Heermance, R. V., and R. Briggs. 2005. Recession of modern glaciers and post-last glacial maximum glacial chronology in the Trinity Alps, CA. Abstracts with Programs No. 37, Geological Society of America, Boulder, CO.

Hershey, O. 1903. The relation between certain river terraces and the glacial series in northwestern California. The Journal of Geology 11:431-458.

Hoffman, M., A. Fountain, and J. Achuff. 2007. 20th-century variations in area of cirque glaciers and glacierets, Rocky Mountain National Park, Rocky Mountains, Colorado, USA. Annals of Glaciology 46:349-354.

Howat, I. M., S. Tulaczyk, P. Rhodes, K. Israel, and M. Snyder. 2006. A precipitation-dominated, mid-latitude glacier system: Mount Shasta, California. Climate Dynamics 28:85-98.

Hubley, R. C. 1956. Glaciers of the Washington Cascade and Olympic Mountains; their present activity and its relation to local climatic trends. Journal of Glaciology 2:669-674.

IPCC. 2013. Climate change 2013. *In* T. F. Stocker, D. Qin, G. K. Plattner, M. Tignor, S. K. Allen, J. Boschung, A. Nauels, Y. Xia, V. Bex, and P. M. Midgley (editors), The Physical Science Basis, Contribution of Working Group I to the Fifth Assessment Report of the Intergovernmental Panel on Climate Change, Cambridge University Press, Cambridge, United Kingdom and New York, NY, USA. Pp. 317-382.

Irwin, W. 1966. Geology of the Klamath Mountains Province. *In* E. Bailey (editor), Geology of Northern California. US Geological Survey, Bulletin 190, California Division of Mines and Geology, San Francisco, CA. Pp. 19-38.

Jackson, K. M., and A. G. Fountain. 2007. Spatial and morphological change on Eliot Glacier, Mount Hood, Oregon, USA. Annals of Glaciology 46:222-226.

Jóhannesson, T., C. Raymond, and E. D. Waddington. 1989. Time-scale for adjustment of glaciers to changes in mass balance. Journal of Glaciology 35:355-369.

Kavanaugh, D., and S. Schoville. 2009. A new and endemic species of *Nebria latreille* (Insecta: Coleoptera: Carabidae: Nebriini), threatened by climate change in the Trinity Alps of northern California. Proceedings of the California Academy of Sciences, Series 4, 60:73-84.

Krimmel R., C. Key, D. Fagre, and R. Menicke. 2002. Glaciers of the conterminous United States—glaciers of the western United States. *In* R. S. Williams Jr, and J. G. Ferrigno (editors), Satellite Image Atlas of Glaciers of the World: North America. US Geological Survey Professional Paper 1386-J-1, US Government Printing Office, Washington, DC.

Kuhn, I. M. 1995. The mass balance of very small glaciers. Zeitschrift für Gletscherkunde und Glazialgeologie Band 31:171-179.

Luo, L., D. Apps, S. Arcand, H. Xu, M. Pan, and M. Hoerling. 2017. Contribution of temperature and precipitation anomalies to the California drought during 2012–2015. Geophysical Research Letters 44:3184-3192.

Matthes, F. E. 1935. Why we should measure our glaciers. Sierra Club Bulletin 20:20-27.

Matthes, F. E. 1940. Committee on glaciers, 1939–1940. Transactions of the American Geophysical Union 1940:396-406.

McKernan, C., D. J. Cooper, and E. W. Schweiger. 2018. Glacial loss and its effect on riparian vegetation of alpine streams. Freshwater Biology 63:518-529.

Meier, M. 1961. Distribution and variations of glaciers in the United States exclusive of Alaska. General Assembly of Helsinki, July 25–August 6, 1960. Commission of Snow and Ice, Gentbrugge 54:420-429.

Meier, M. F. 1984. Contribution of small glaciers to global sea level. Science 226:1418-1421.

Menounos, B., R. Hugonnet, D. Shean, A. Gardner, I. Howat, E. Berthier, B. Pelto, C. Tennant, J. Shea, M. Noh, F. Brun, and A. Dehecq. 2018. Heterogeneous changes in western North American glaciers linked to decadal variability in zonal wind strength. Geophysical Research Letters 46:200-2009.

Milner, A., K. Khamis, T. Battin, J. Brittain, N. Barrand, L. Füreder, S. Cauvy-Fraunié, G. Már Gíslason, D. Jacobsen, D. Hannah, A. Hodson, E. Hood, V. Lencioni, J. Ólafsson, C. Robinson, M. Tranter, and L. Brown. 2017. Glacier shrinkage effects on downstream systems. Proceedings of the National Academy of Sciences 114:9770-9778.

Moore, J. G., and B. C. Moring. 2013. Rangewide glaciation in the Sierra Nevada, California. Geosphere 9:1804-1818.

Mote, P. W., A. F. Hamlet, M. P. Clark, and D. P. Lettenmaier. 2005. Declining mountain snowpack in western North America. American Meteorological Society 86:39-49.

Mote, P. W., S. Li, D. P. Lettenmaier, M. Xiao, and R. Engel. 2018. Dramatic declines in snowpack in the western US. Npj Climate and Atmospheric Science 1:2.

Moyle, P. B. 2002. Inland Fishes of California. Regents of the University of California, Berkeley, CA.

Nakamoto, R. J. 1994. Characteristics of pools used by adult summer steelhead oversummering in the New River, California. Transactions of the American Fisheries Society 123:757-765.

Nye, J. F. 1960. The response of glaciers and ice-sheets to seasonal and climatic changes: Proceedings of the Royal Society of London. Series A. Mathematical and Physical Sciences 256:559-584.

Nylen, T. 2004. Spatial and temporal variations of glaciers on Mount Rainier between 1913 and 1994. M.S. Thesis, Portland State University, Portland, OR.

Olson, D., D. A. DellaSala, R. F. Noss, J. R. Strittholt, J. Kass, M. E. Koopman, and T. F. Allnutt. 2012. Climate change refugia for biodiversity in the Klamath-Siskiyou ecoregion. Natural Areas Journal 32:65-74.

O'Neel, S., E. Hood, A. L. Bidlack, S. W. Fleming, M. L. Arimitsu, A. Arendt, E. Burgess, C. J. Sergeant, A. H. Beaudreau, K. Timm, G. D. Hayward, J. H. Reynolds, and S. Pyare. 2015. Icefield-to-ocean linkages across the northern Pacific coastal temperate rainforest ecosystem. BioScience 65:499-512.

O'Neel, S. C. McNeil, L. C. Sass, C. Florentine, E. H. Baker, E. Peitzsch, D. McGrath, A. G. Fountain, and D. Fagre. 2019. Reanalysis of the US Geological Survey Benchmark Glaciers: long-term insight into climate forcing of glacier mass balance. Journal of Glaciology 65:850-866.

Osborn, G., B. Menounos, C. Ryane, J. Riedel, J. Clague, J. Koch, D. Clark, K. Scott, and P. Davis. 2012. Latest Pleistocene glacier fluctuations on Mount Baker, Washington. Quaternary Science Reviews 49:33-51.

Pelto, M. 2018. How unusual was 2015 in the 1984–2015 period of the North Cascade Glacier annual mass balance? Water 10:543.

PRISM Climate Group. 2018. Spatial climate dataset. Oregon State University, Corvallis. Available online at http://prism.oregonstate.edu (accessed 06 November 2018).

Radić, V., A. Bliss, A. C. Beedlow, R. Hock, E. Miles, and J. G. Cogley. 2013. Regional and global projections of 21st century glacier mass changes in response to climate scenarios from global climate models. Climate Dynamics 42:37-58.

Raper, S. C., and R. J. Braithwaite. 2009. Glacier volume response time and its links to climate and topography based on a conceptual model of glacier hypsometry. The Cryosphere 3:183-194.

Raub, W. B., C. S. Brown, and A. Post. 2006. Inventory of glaciers in the Sierra Nevada, California. US Geological Survey Open File Report, 2006-1239. US Geological Survey, Reston, VA.

Rhodes, P. T. 1987. Historic glacier fluctuations on Mount Shasta, Siskiyou County, California Geology 40:205-211.

Riedel, J. L., and M. A. Larrabee. 2016. Impact of recent glacial recession on summer streamflow in the Skagit River. Northwest Science 90:5-22.

Riedel J., S. Wilson., W. Baccus, M. Larrabee, T. Fudge, and A. Fountain. 2015. Glacier status and contribution to streamflow in the Olympic Mountains, Washington, USA. Journal of Glaciology 61:8-16.

Robinson, C. T., U. Uehlinger, and M. Hieber. 2001. Spatio-temporal variation in macroinvertebrate assemblages of glacial streams in the Swiss Alps. Freshwater Biology 46:1663-1672.

Sawyer, J. O. 2006. Northwest California: A Natural History. University of California Press, Berkeley, CA.

Schoville, S. D., and G. O. Graening. 2013. Updated checklist of the ice-crawlers (Insecta: Grylloblattodea: Grylloblattidae) of North America, with notes on their natural history, biogeography and conservation. Zootaxa 3737:351-378.

Sharp, R. 1960. Pleistocene glaciation in the Trinity Alps of northern California. American Journal of Science 258:305-340.

Sitts, D. J., A. G. Fountain, and M. J. Hoffman. 2010. Twentieth century glacier change on Mount Adams, Washington, USA. Northwest Science 84:378-385.

Shook, K., and D. Gray. 1997. Synthesizing shallow seasonal snow covers. Water Resources Research 33:419-426.

Shukla, S., M. Safeeq, A. AghaKouchak, K. Guan, and C. Funk. 2015. Temperature impacts on the water year 2014 drought in California. Geophysical Research Letters 42:4384-4393.

Skinner, C. N., A. H. Taylor, and J. K. Agee. 2006. Klamath Mountains Bioregion. *In* J. W. van Wagtendonk, J. Fites-Kaufmann, K. E. Shaffer, A. E. Thode, and N. S. Sugihara (editors), Fire in California's Ecosystems, University of California Press, Berkeley. Pp. 170-194.

Solomina, O. N., R. S. Bradley, V. Jomelli, A. Geirsdottir, D. S. Kaufman, J. Koch, N. P. McKay, M. Masiokas, G. Miller, A. Nesje, K. Nicolussi, L. A. Owen, A. E. Putnam, H. Wanner, G. Wiles, and B. Yang. 2016. Glacier fluctuations during the past 2000 years. Quaternary Science Review 149:61-90.

Thompson, D. W. J., J. M. Wallace, J. J. Kennedy, and P. D. Jones. 2010. An abrupt drop in Northern Hemisphere sea surface temperature around 1970. Nature 467:444-447.

Thomson, R. C., A. N. Wright, and H. B. Shaffer. 2016. California Amphibian and Reptile Species of Special Concern. University of California Press, Oakland, CA.

Ullrich, P. A., Z. Xu, A. M. Rhoades, M. D. Dettinger, J. F. Mount, A. D. Jones, and P. Vahmani. 2018. California's drought of the future: A midcentury recreation of the exceptional conditions of 2012–2017. Earth's Future 6:1568-1587.

Westerling, A. L., H. G. Hidalgo, D. R. Cayan, and T. W. Swetnam. 2006. Warming and earlier spring increase Western US forest wildfire activity. Science 313:940-943.

Williams, A. P., R. Seager, J. T. Abatzoglou, B. I. Cook, J. E. Smerdon, and E. R. Cook. 2015. Contribution of anthropogenic warming to California drought during 2012–2014. Geophysical Research Letters 42:6819-6828.

Zemp, M., H. Frey, I. Gärtner-Roer, S. U. Nussbaumer, M. Hoelzle, F. Paul, W. Haeberli, F. Denzinger, A. P. Ahlstrøm, B. Anderson, S. Bajracharya, C. Baroni, L. N. Braun, B. E. C. Ceres, G. Casassa, G. Cobos, R. R. D. Vila, H. Delgado Granados, M. N. Demuth, L. Espizua, A. Fischer, K. Fujita, B. Gadek, A. Ghazanfar, J. O. Hagen, P. Holmlund, N. Karimi, Z. Li, M. Pelto, P. Pitte, V. V. Popovnin, C. A. Portocarrero, R. Prinz, C. V. Sangewar, I. Severskiy, O. Sigurdsson, A. Soruco, R. Usubaliev, and C. Vincent. 2015. Historically unprecedented global glacier decline in the early 21st century. Journal of Glaciology 61:745-762.

Zemp, M., M. Huss, E. Thibert, N. Eckert, R. McNabb, J. Huber, M. Barandun, H. Machguth, S. U. Nussbaumer, I. Gärtner Roer, L. Thomson, F. Paul, F. Maussion, S. Kutuzov, and J. G. Cogley. 2019. Global glacier mass changes and their contributions to sea-level rise from 1961 to 2016. Nature 568:382-386.

Supplemental material available online at http://www.bioone.org/loi/nwsc

Received 09 June 2019
Accepted 21 October 2019